Geoderma 452 (2024) 117108

Contents lists available at ScienceDirect

Geoderma

journal homepage: www.elsevier.com/locate/geoderma

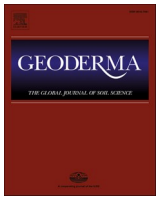

Carbon dioxide exchange and temperature sensitivity of soil respiration along an elevation gradient in an arctic tundra ecosystem

Wenyi Xu [a,b,*], Andreas Westergaard-Nielsen [b], Anders Michelsen [c], Per Lennart Ambus [b]

[a] Department of Soil and Environment, Swedish University of Agricultural Sciences, Sweden
[b] Department of Geosciences and Natural Resource Management, University of Copenhagen, Denmark
[c] Department of Biology, University of Copenhagen, Denmark

ARTICLE INFO

Handling Editor: C. Rumpel

Keywords:
Net ecosystem exchange
Ecosystem respiration
Gross ecosystem production
Temperature sensitivity
Moisture sensitivity
Soil nutrients

ABSTRACT

Generally, with increasing elevation, there is a corresponding decrease in annual mean air and soil temperatures, resulting in an overall decrease in ecosystem carbon dioxide (CO_2) exchange. However, there is a lack of knowledge on the variations in CO_2 exchange along elevation gradients in tundra ecosystems. Aiming to quantify CO_2 exchange along elevation gradients in tundra ecosystems, we measured ecosystem CO_2 exchange in the peak growing season along an elevation gradient (9–387 m above sea level, m.a.s.l) in an arctic heath tundra, West Greenland. We also performed an *ex-situ* incubation experiment based on soil samples collected along the elevation gradient, to assess the sensitivity of soil respiration to changes in temperature and soil moisture. There was no apparent temperature gradient along the elevation gradient, with the lowest air and soil temperatures at the second lowest elevation site (83 m). The lowest elevation site exhibited the highest net ecosystem exchange (NEE), ecosystem respiration (ER) and gross ecosystem production (GEP) rates, while the other three sites generally showed intercomparable CO_2 exchange rates. Topography aspect-induced soil microclimate differences rather than the elevation were the primary drivers for the soil nutrient status and ecosystem CO_2 exchange. The temperature sensitivity of soil respiration above 0 °C increased with elevation, while elevation did not regulate the temperature sensitivity below 0 °C or the moisture sensitivity. Soil total nitrogen, carbon, and ammonium contents were the controls of temperature sensitivity below 0 °C. Overall, our results emphasize the significance of considering elevation and microclimate when predicting the response of CO_2 balance to climate change or upscaling to regional scales, particularly during the growing season. However, outside the growing season, other factors such as soil nutrient dynamics, play a more influential role in driving ecosystem CO_2 fluxes. To accurately upscale or predict annual CO_2 fluxes in arctic tundra regions, it is crucial to incorporate elevation-specific microclimate conditions into ecosystem models.

1. Introduction

Climate change is occurring rapidly in the Arctic, where air temperature has been increasing at rates more than three times the global average and precipitation has increased by 9 % in the past 50 years (Rantanen et al., 2022). These trends have induced significant changes in tundra ecosystems across the Arctic, such as plant productivity, organic matter decomposition and soil nutrient availability (Ravn et al., 2020; Xu et al., 2021b; Heijmans et al., 2022). Of great concern is that the very large soil organic carbon (C) pools located in arctic tundra may cause a substantial release of carbon dioxide (CO_2) as climate warms. Tundra ecosystems are exposed to different air and soil temperature, soil moisture, and nutrient regimes along elevation gradients (Oberbauer et al., 2007). Uplands typically experience cooler air and soil temperatures, while low-lying areas may have warmer temperatures and higher soil moisture (Paré and Bedard-Haughn, 2012). Such differences may lead to large variations in plant productivity and soil microbial activities, and thereby the exchange of CO_2 between soil and atmosphere.

With increasing elevation, there is a corresponding decrease in mean annual air and soil temperatures, resulting in an overall decrease in net ecosystem exchange (NEE), gross ecosystem production (GEP) and ecosystem respiration (ER) (Garten and Hanson, 2006; Zona et al., 2011). However, the way temperature changes with elevation can be affected by wind. When wind blows up a mountain slope, it can cause

* Corresponding author at: Department of Geosciences and Natural Resource Management, University of Copenhagen, Denmark
E-mail address: wexu@ign.ku.dk (W. Xu).

https://doi.org/10.1016/j.geoderma.2024.117108
Received 29 September 2023; Received in revised form 20 May 2024; Accepted 11 November 2024
Available online 19 November 2024

the air to cool at a faster rate than the dry adiabatic lapse rate (Córdova et al., 2016). Wind also has impacts on the aerodynamic boundary layer, which can in turn affect the convective heat loss, evaporative cooling and distribution of snow, and thus microclimates above and below the soil surface (Körner, 2021). Hence, in arctic tundra ecosystems where strong winds are common, the exchange of CO_2 may not vary across elevation gradients in the same way as other less windy ecosystems (Rodeghiero and Cescatti, 2005; Zeeman et al., 2010; Whitaker et al., 2014; Flerchinger et al., 2020). However, there is still a poor understanding of the variations in CO_2 exchange along elevation gradients in tundra ecosystems.

Soil respiration is the largest contributor to C effluxes from tundra ecosystems to the atmosphere (Watts et al., 2021), and its response to temperature plays a key role in regulating feedbacks associated with climate warming. Soil respiration in cold climates is considerably more sensitive to temperature compared with warmer regions (Carey et al., 2016). The temperature sensitivity (commonly referred to as Q_{10}) in arctic tundra soils has been reported to primarily depend on the quantity and quality of C, soil temperatures and water content (Elberling, 2007; Bauer et al., 2012). For example, Boddy et al. (2008) found the turnover of low molecular weight dissolved organic C pools to be less sensitive to temperature compared with higher molecular weight C pools in high arctic tundra soils. Microbial activity is known to occur under frozen conditions in arctic tundra soil, leading to significant cumulative CO_2 efflux rates during winter (Panikov et al., 2006; Morgner et al., 2010). However, the interactions between temperature and soil microbial respiration have mainly been assessed within the 0–30 °C range (Schindlbacher et al., 2010; Richardson et al., 2012; Dan et al., 2016; Nottingham et al., 2019), with a few studies characterizing CO_2 efflux below 0 °C (Mikan et al., 2002; Elberling and Brandt, 2003). Moreover, several studies across various ecosystems (such as Mediterranean and Alpine grasslands and tropical and boreal forests) have reported an increase in the temperature sensitivity of soil respiration with elevation (Vanhala et al., 2008; Gutiérrez-Girón et al., 2015; Nottingham et al., 2019). Whether the increase in temperature sensitivity is rather an effect of elevation-induced variations in C and nutrient availability, or reflects the general phenomenon of higher temperature sensitivity under lower soil temperature regimes is still under debate (Schindlbacher et al., 2010). Although several studies have investigated temperature sensitivity along latitude gradients in the Arctic, these results can be influenced by contrasting parent materials and soil types (Kim et al., 2013; Karhu et al., 2014; Kobayashi et al., 2016). In contrast, elevation gradients offer a unique advantage, as they typically encompass consistent parent materials and soil types, thereby eliminating the potential influence of these factors on temperature sensitivity. However, little is known about how temperature sensitivity of respiration varies along elevation gradients, and information on temperature sensitivity below 0 °C is even sparser.

Soil moisture availability is also a crucial factor influencing soil respiration. Generally, soil respiration increases with increasing moisture content at the lower range of soil moisture but tends to slow down or decrease when soil moisture inhibits oxygen diffusion (Moyano et al., 2013). Elevation affects soil moisture variability through impact on precipitation patterns, snow accumulation, wind, and the downward movement of water (Knowles et al., 2015). For example, the melting of frozen soil water and snow from uplands can cause the accumulation of water in low-lying areas, creating saturated-anaerobic conditions that inhibit soil respiration. Azizi-Rad et al. (2022) found that moisture sensitivity of soil respiration was higher under nearly dry and under anoxic conditions and they suggested microbial activity and respiration may require more energy in these extremes to occur. Thus, it is likely the contrasting moisture conditions across elevation gradients can result in different responses of soil respiration to changes in moisture content. Indeed, the moisture sensitivity of soil respiration has been found to increase with elevation in subtropical forests (Ma et al., 2019). However, experimental data for moisture sensitivity along elevation gradients in arctic tundra are lacking.

In this study, we measured ecosystem CO_2 exchange and sensitivity of soil respiration to changes in temperature and soil moisture along an elevation gradient (387 m) in an arctic heath tundra, West Greenland. The underlying hypotheses are that: (H1) air and soil temperatures and soil nutrient availability decrease with increasing elevation; (H2) ecosystem CO_2 exchange rates decrease with increasing elevation; and (H3) the sensitivity of soil respiration to temperature and moisture increases with increasing elevation, due to decreasing soil temperatures and soil moisture content.

2. Materials and methods

2.1. Study sites

This study was conducted on the south of Disko Island, West Greenland, in the transition zone between the Low and High Arctic. The study area has a typical Low Arctic climate, with an annual mean air temperature of -3 ± 1.8 °C and an annual mean precipitation of 418 ± 131 mm. Underlain by discontinuous permafrost, the area has a thin organic soil layer (5–10 cm) on the top of mineral soil dominated by coarse basaltic rock sand and gravel sediments formed within the last 10.000 years. The soil is classified as Haplic Cryosol according to the World Reference Base for Soil Resources. Four study sites were chosen in this study based on their elevation in meters above sea level (m.a.s.l.) ranging from 9 to 387 m.a.s.l. The lowest tundra site is at Østerlien, next to Arctic station, 9 m.a.s.l. and SE-SW facing (S_9), and the second lowest site is located at Blæsedalen at an elevation of 83 m.a.s.l and NE-SW facing (S_{83}). The second highest and highest sites are at the S-SW facing mountainside of Skarvefjeldet at elevations of 240 (S_{240}) and 387 m.a.s.l (S_{387}), respectively. The S_9 site has shelter from all directions except from South and is situated in a little valley-like area. The S_{83} site is more exposed to winds, as it only gets shelter from East and is situated on more open terrain. The S_{240} and S_{387} sites are sloping and also exposed to winds, but sheltered towards N-NE. The detailed information for each site in terms of coordinates, elevation, slope and aspect can be found in Table S1. The four sites, situated within a horizontal distance of 3400 m, have similar vegetation cover and composition with heath tundra characteristics (Table S2) encompassing a moss layer, a mixture of herbaceous species, and prostrate or hemiprostrate dwarf shrubs. The dominant plant species are deciduous dwarf shrubs e.g. bog bilberry (*Vaccinium uliginosum),* dwarf birch (*Betula nana),* grey willow (*Salix glauca*), evergreen low shrubs black crowberry (*Empetrum hermaphroditum*) and Arctic bell-heather (*Cassiope tetragona*), and a mixture of scattered graminoids with a canopy height typically <15 cm (Table S2).

2.2. Measurement of carbon dioxide fluxes

The four study sites had the same experimental set up. For each site, six replicate plots of 1 × 1 m were established adjacent to each other, with stainless steel collars permanently installed to 5 cm soil depth. The current design with six replicates, as a compromise between resource constraints and logistical feasibility, is aligned with numerous other studies in similar environments (Virkkala et al., 2018). The collars were preinstalled in plots with vegetation covers that appeared representative for the particular site (see photo in Fig. S1). Surface CO_2 fluxes were measured using a static chamber technique. For gas flux measurements, a transparent polycarbonate chamber (21 × 21 × 19.5 cm) was mounted in a water-filled groove atop the collars to establish a gas-tight seal between chamber enclosure and outside atmosphere. At each site, the CO_2 flux measurements were conducted four times (i.e., July 26th, August 7th, August 12th and August 18th) in the summer of 2017. Due to logistical limitations, the measurements were done at different time of day across the sites. However, at this northern location and at this time of year, midnight sun prevails and diurnal fluctuations in soil temperatures are accordingly dampened. During each campaign, each plot was

measured twice by using a CO_2 infrared gas analyzer (EGM-5, PP System, Amesbury, USA). The first measurement was performed under light condition using the transparent chamber to establish net ecosystem exchange (NEE). The second measurement was taken under dark conditions using the chamber covered by a black cloth to establish ecosystem respiration (ER). The CO_2 concentrations were measured and recorded at a 1 s sampling frequency during a 5 min chamber closure time. The CO_2 fluxes were estimated as the slope of the linear regression ($p < 0.05$, $R^2 > 0.9$) of the changes in CO_2 concentrations over time. Gross ecosystem photosynthesis (GEP) was calculated as the difference between ER and NEE rates.

Along with gas measurements, soil temperature and soil moisture were manually recorded in triplicates within each plot next to the collar. Soil temperature and soil volumetric moisture (%vol) at 5 cm depth were measured with a HI93503 (Hanna Instruments, Woonsocket, RI, USA) and a ML2X Theta Probe coupled to a HH2 Moisture Meter (Delta-T Devices, Cambridge, UK), respectively. Normalized difference vegetation index (NDVI) was measured in triplicates 30 cm above the surface within each plot by using a SKR 10 sensor (Skye instruments, Powys, UK). Photosynthetically active radiation (PAR) was measured with a Sun System PAR Meter with Remote Sensor.

2.3. Soil sampling and analysis

On July 26th and August 12th, 2017, 2 or 3 replicate soil samples were collected in the top 0–10 cm soil in each plot at each site with a 2-cm-diameter auger, and then split into 0–5 cm and 5–10 cm soil depth. The replicate samples were subsequently mixed thoroughly into one composite sample. Coarse roots and stones were removed by hand, and soil moisture was calculated from oven drying weight loss (105 °C, 24 h). Total soil C and N contents as well as $^{13}C/^{12}C$ and $^{15}N/^{14}N$ isotopic ratios were measured by an elemental analyzer (CE1110, Thermo Electron, Milan, Italy) coupled in continuous flow mode to a Finnigan MAT Delta PLUS isotope ratio mass spectrometer (IRMS; Thermo Scientific, Bremen, Germany). Prior to analysis, 20–30 mg of dry and finely ground soil was placed in tin cups and subsequently folded. Soil pH was determined in 1:2.5 (weight: volume) soil: water suspension with a handheld pH meter (3210, WTW). Soil extractions were made by suspending field moist soil in deionized water (10 g soil; 50 mL water), shaking for 1 h at room temperature terminated by filtration through 2.7 μm membrane filter (Whatman GF/D). Filtrates were kept frozen until analysis for ammonium (NH_4^+-N), nitrate (NO_3^--N) and phosphate (PO_4^{3-}-P) using flow-injection analysis (Tecator 5000 FIAStar, Höganäs, Sweden). Soil dissolved organic C (DOC) and total dissolved N (TDN) in the filtered extracts were measured using a TOC-TN analyzer (Shimadzu, Kyoto, Japan). Dissolved organic N (DON) was calculated as the difference between TDN and dissolved inorganic N (NO_3^--N + NH_4^+-N).

2.4. Air temperature and soil temperature

Air temperature, and soil temperature loggers were installed in the vicinity of the soil collars at each site, recording the air temperature in 30 cm height and soil temperature and moisture in both 2 cm and 5 cm depths at 10 min intervals. The loggers were in place during the study. Long-term air temperature data (at 2 m height) were available from four weather stations placed at <100 m distance from each of the four study sites. Ground surface temperature data were recorded at the S_9 and S_{387} sites.

2.5. Incubation experiment

An incubation experiment was conducted to investigate the responses of soil respiration to changes in temperatures and soil moisture contents. On August 5th, 2017, soil samples were collected in the top 0–3.5 cm depth from all the plots, with a 6-cm-diameter steel cylinder. The intact soil cores were transferred into 2-L jars (with lids, inlet and outlet values), and placed in an adjustable freezer at a given temperature. A wetted piece of paper towel was put at the bottom of each jar to keep the samples from drying out. The measurement of soil respiration was conducted by closing the jars air-tightly and connecting in a closed loop mode to the CO_2 infrared gas analyzer.

For the temperature response assessment, soil respiration was measured under 8 different temperatures both above (at 2 °C, 5 °C, 10 °C and 15 °C) and below 0 °C (at −10 °C, −7 °C, −2 °C and 0 °C). For incubations above the freezing point jar CO_2 concentration was measured every hour for around 3 h after the jar closure (4–5 time points), while below the freezing point jar CO_2 concentration was measured every 6 h for around 18 h to reduce the disturbance on the freezing samples (3–4 time points).

For the moisture response assessment, soil respiration was measured at 5 °C without water addition and hereafter measured under the same temperature but with water addition. Each sample was added with the same amount of water (2.5 or 5 mL) each time until the samples began to drain (in total 11 times). Each time water was added, jar CO_2 concentration was measured immediately after the jar closure and again after 5–6 h (2 time points).

The jar CO_2 concentration was analyzed at each time point by deployment of the gas monitor for 30 s, and soil respiration subsequently was estimated as the slope of the linear regression ($p < 0.05$, $R^2 > 0.9$) of the changes in CO_2 concentrations over time.

2.6. Calculations and statistics

The correlation between soil respiration and temperature (above 0 °C) was fitted by a linear regression, while the correlation for the temperature below 0 °C was fitted by an exponential regression. The temperature sensitivity (Q_{10}) of soil respiration (above 0 °C) was calculated with the equation ($Q_{10} = \frac{K2}{K1}^{(\frac{10}{T2-T1})}$) from Findlay et al. (2015), and the Q_{10} value (below 0 °C) was estimated by the equation (respiration $= ae^{\beta T}$, where $Q_{10} = e^{(\beta \times 10)}$) from Davidson et al. (2006). The relationship between soil respiration and soil (volumetric) moisture content was fitted by a quadratic regression. Also, the data before the point at which soil respiration peaked were fitted by a linear regression. The slope of the regression line represented the moisture sensitivity of soil respiration (Zhang et al., 2015; Ma et al., 2019). Considering that each soil sample started with different soil moisture content (before adding water), we normalized soil respiration rates for each sample (being converted to the ratio of specific soil respiration to the maximum soil respiration for each sample).

Prior to statistical analysis, we inspected the QQ-plots (quantile–quantile plots) and used Shapiro-Wilk normality test and Levene's test to check data for normal distribution and homogeneity of variance, and data were log or square root transformed when necessary. To test the hypotheses (I-III), we tested site differences in soil chemical properties (C, N, C:N, NO_3^--N, NH_4^+-N, DON, DOC, total P, PO_4^{3-}-P, pH, $\delta^{13}C$ and $\delta^{15}N$), soil moisture and temperature, surface CO_2 fluxes, and temperature (Q_{10}) and moisture sensitivity. Site differences were tested separately (within each campaign or at each soil depth) or in combined campaigns (repeated measurement analysis) by using one-way ANOVA model. Post hoc pairwise comparisons between levels of the significant factor were then conducted using the emmeans package, with Tukey's Honestly Significant Differences (Tukey HSD) p-value adjustment (Lenth, 2020). The significant site differences are based on $p \leq 0.05$. To explore the relationship between normalized soil respiration and soil moisture content (water filled pore space WFPS), a linear regression was applied for each site. To explore the main drivers of surface CO_2 fluxes, the correlations between surface CO_2 fluxes, and soil temperature, soil moisture, NDVI and PAR were examined by multiple stepwise regression analysis (based on 4 sites × 3 or 4 campaigns × 6 replicates). To explore the correlations between temperature and moisture sensitivity, and soil physicochemical properties, Pearson correlation analysis (based on 4

sites × 6 replicates) was performed by using the psych package (Revelle and Revelle, 2015). Furthermore, to quantify the comprehensive relationship between temperature and moisture sensitivity, and soil physicochemical properties, principal component analysis (PCA) (based on 4 sites × 2 campaigns × 6 replicates) was applied by using the prcomp package (Mankin, 2008). All analyses above were performed using R software v. 3.6.1 (Team, 2019).

3. Results

3.1. Air temperature, soil temperature and soil moisture

Continuous temperature observations showed that air temperatures in 30 cm height at the two high elevation sites fluctuated considerably during the measurement period, ranging from 3.5 °C to 15.3 °C at the S_{240} site and from 1.7 °C to 16.2 °C at the S_{387} site, while the S_{83} site generally had relatively stable air temperatures (Fig. 1a). In the period between August 5th and August 18th, the S_{83} site was coolest (a mean daily temperature of 7.6 °C) and the S_{240} site had a relatively high daily temperature (9.4 °C; Fig. 1a). The long-term air temperature data (from 2016 to 2017) showed that the S_{83} site was coolest (a mean annual temperature of –3.5 °C) and the S_9 site was the warmest (a mean annual temperature of −1.8 °C; Fig. 2). The S_9 and S_{387} sites had mean annual ground temperatures of −3.8 °C and −3.6 °C, respectively, from 2015 to 2017 (Fig. S2).

The lowest mean daily soil temperatures were observed at the S_{83} site for both depths (6.9 °C and 5.9 °C at 2.5 cm and 5 cm depths, respectively), while the S_9 and S_{387} sites had the highest soil temperatures at 2.5 cm (10.1 °C) and 5 cm depths (9.3 °C), respectively (Fig. 1b and c). When comparing soil temperatures between sites, the S_{83} site was significantly cooler than the other three sites at 2.5 cm depth ($p < 0.05$; Fig. 1b). At 5 cm depth, all the sites significantly differed from each other ($p < 0.01$), except for the S_9 and S_{240} sites, which had similar soil temperatures (Fig. 1c). The manually measured soil moisture data showed that the lowest site (S_9) had the highest soil moisture content, while the other three sites had similar soil moisture content (Fig. 1d).

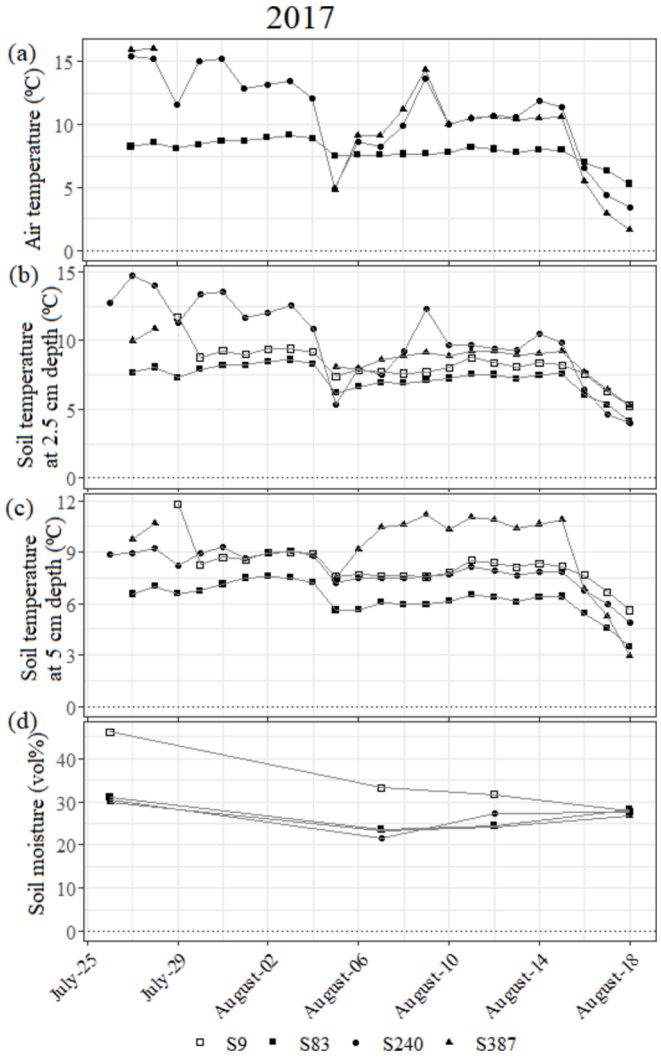

Fig. 1. Daily mean air temperature at 30 cm height (a), soil temperature at 2.5 cm depth (b), soil temperature at 5 cm depth (c), and manually measured soil moisture (d) in 2017 from the four study sites in Disko Island, West Greenland along an elevation gradient. Site names reflect altitude in meters above sea level.

3.2. Soil chemical properties

Basic soil chemical properties at the four sites are shown in Table 1. Total soil C and N contents did not significantly vary among study sites, while total soil P contents varied significantly among sites at both depths ($p < 0.01$; Table1). Soil C: N ratio was significantly lower at the S_9 site than the S_{83} and S_{387} sites at 0–5 cm depth ($p < 0.05$), and at the 5–10 cm depth the S_{387} site exhibited significantly higher ratio than the other three sites ($p < 0.05$; Table 1).

There were significant variations in soil DOC and DON concentrations between sites or dates. On July 27th, the highest DOC and DON concentrations in top 5 cm were both observed at the S_{240} site, being 2-fold to 6-fold higher than the other two lower elevation sites (S_9 and S_{83}, $p < 0.05$; Table1). At 5–10 cm soil depth, the highest elevation site (S_{387}) had significantly higher DOC concentrations than the other three sites ($p < 0.05$), and 3-fold higher DON concentrations than the S_{83} site ($p = 0.004$; Table 1). On August 12th, the highest DOC concentrations at both depths were observed at the S_{387} site, but they only significantly differed at 0–5 cm soil depth ($p < 0.05$; Table 1). In contrast, the highest DON concentrations at both depths were observed at the lowest elevation site (S_9), being 2-fold higher than the concentrations at the S_{83} site ($p = 0.029$; Table 1).

Soil NO_3^--N and NH_4^+-N concentrations at both depths differed between sites ($p < 0.05$; Table 1). Soil NO_3^--N concentrations at both depths were generally the highest at the lowest elevation site (S_9), while the highest soil NH_4^+-N concentrations were observed at the relatively high elevation site (either the S_{240} or S_{387} site).

Soils collected from all the four sites at both depths were slightly

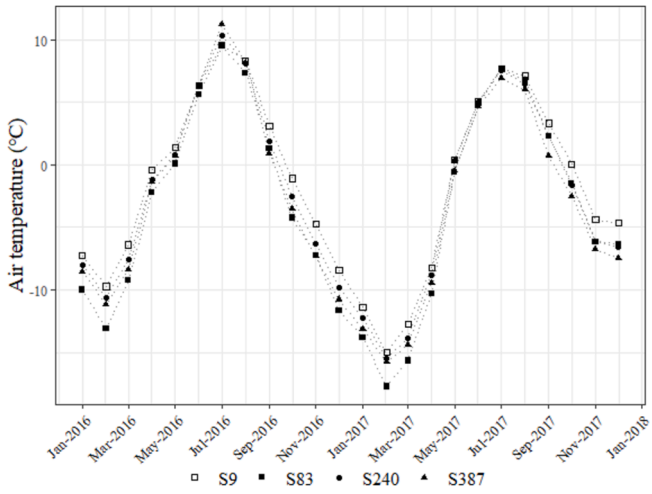

Fig. 2. Monthly air temperature at 2 m height over the period of 2016–2017 from the weather stations near each site (<100 m).

Table 1
Soil physicochemical properties from the four study sites in Disko Island, West Greenland.

	Date	Soil depth	Site S_9	S_{83}	S_{240}	S_{387}
C (%)[§]		0–5 cm	13.5 ± 2.0	11.7 ± 1.3	17.3 ± 2.5	11.9 ± 0.8
		5–10 cm	7.0 ± 1.6	3.4 ± 0.4	6.9 ± 1.1	5.5 ± 0.3
N (%)[§]		0–5 cm	0.7 ± 0.1	0.5 ± 0.1	0.8 ± 0.1	0.5 ± 0.0
		5–10 cm	0.5 ± 0.1	0.3 ± 0.0	0.5 ± 0.1	0.3 ± 0.0
C:N[§]		0–5 cm	17.7 ± 0.7^{a}	21.3 ± 1.1^{b}	20.7 ± 0.7^{ab}	23.5 ± 0.9^{b}
		5–10 cm	13.1 ± 0.3^{a}	13.3 ± 0.4^{a}	14.7 ± 0.5^{a}	16.5 ± 0.5^{b}
Total P (g kg^{-1})	July 27th	0–5 cm	0.8 ± 0.1^{b}	0.3 ± 0.0^{a}	0.7 ± 0.0^{b}	1.1 ± 0.0^{c}
		5–10 cm	0.7 ± 0.1^{b}	0.4 ± 0.1^{a}	0.7 ± 0.1^{b}	0.9 ± 0.1^{b}
DOC (mg kg^{-1})	July 27th	0–5 cm	27.1 ± 22.5^{a}	60.9 ± 29.9^{a}	198.3 ± 51.2^{b}	113.0 ± 19.0^{ab}
		5–10 cm	1.0 ± 0.6^{a}	0^{a}	1.9 ± 1.6^{a}	26.9 ± 15.2^{b}
	August 12th	0–5 cm	54.4 ± 4.4^{a}	45.3 ± 11.0^{a}	71.1 ± 16.3^{a}	115.0 ± 40.1^{b}
		5–10 cm	14.8 ± 7.6	0	0	16.0 ± 9.5
DON (mg kg^{-1})	July 27th	0–5 cm	22.2 ± 7.8^{a}	20.8 ± 3.9^{a}	50.6 ± 10.3^{b}	24.6 ± 3.7^{ab}
		5–10 cm	12.2 ± 3.6^{ab}	4.9 ± 0.6^{a}	8.6 ± 1.8^{ab}	15.4 ± 3.6^{b}
	August 12th	0–5 cm	20.7 ± 2.0^{b}	11.1 ± 1.3^{a}	13.9 ± 2.9^{ab}	15.1 ± 2.5^{ab}
		5–10 cm	9.9 ± 2.1^{b}	5.0 ± 0.9^{a}	5.7 ± 1.1^{ab}	8.2 ± 1.5^{ab}
NO_3^--N (mg kg^{-1})	July 27th	0–5 cm	0.12 ± 0.02^{ab}	0.06 ± 0.01^{a}	0.16 ± 0.02^{b}	0.12 ± 0.02^{ab}
		5–10 cm	0.41 ± 0.06^{b}	0.08 ± 0.03^{a}	0.09 ± 0.02^{a}	0.07 ± 0.01^{a}
	August 12th	0–5 cm	0.09 ± 0.02^{b}	0.04 ± 0.00^{a}	0.07 ± 0.01^{ab}	0.05 ± 0.00^{a}
		5–10 cm	0.14 ± 0.03^{c}	0.05 ± 0.01^{ab}	0.08 ± 0.01^{bc}	0.04 ± 0.01^{a}
NH_4^+-N (mg kg^{-1})	July 27th	0–5 cm	0.70 ± 0.20^{a}	0.37 ± 0.17^{a}	4.53 ± 1.03^{b}	0.53 ± 0.11^{a}
		5–10 cm	0.30 ± 0.12^{a}	0.02 ± 0.01^{a}	0.29 ± 0.10^{a}	1.13 ± 0.33^{b}
	August 12th	0–5 cm	0.52 ± 0.10^{ab}	0.17 ± 0.05^{a}	0.59 ± 0.20^{ab}	0.81 ± 0.14^{b}
		5–10 cm	0.07 ± 0.04^{a}	0.05 ± 0.07^{a}	0.06 ± 0.03^{a}	0.38 ± 0.18^{b}
PO_4^{3-}-P (mg kg^{-1})	July 27th	0–5 cm	0.28 ± 0.03	0.63 ± 0.43	0.28 ± 0.05	0.23 ± 0.08
		5–10 cm	0.24 ± 0.12	0.07 ± 0.01	0.16 ± 0.04	0.13 ± 0.03
	August 12th	0–5 cm	0.37 ± 0.10	0.21 ± 0.05	0.40 ± 0.11	0.36 ± 0.12
		5–10 cm	0.17 ± 0.04	0.11 ± 0.02	0.12 ± 0.03	0.11 ± 0.03
pH	July 27th	0–5 cm	6.20 ± 0.08	6.19 ± 0.13	6.09 ± 0.09	5.99 ± 0.10
		5–10 cm	6.45 ± 0.10^{b}	6.50 ± 0.03^{ab}	6.35 ± 0.05^{ab}	6.20 ± 0.05^{a}
	August 12th	0–5 cm	6.48 ± 0.03^{b}	6.03 ± 0.09^{ab}	6.31 ± 0.09^{ab}	6.22 ± 0.10^{a}
		5–10 cm	6.64 ± 0.14	6.60 ± 0.13	6.55 ± 0.08	6.42 ± 0.05
Gravimetric water content (%)	July 27th	0–5 cm	66.8 ± 9.6b	44.5 ± 7.6^{ab}	50.7 ± 8.5^{ab}	36.2 ± 3.8^{a}
		5–10 cm	56.4 ± 15.1^{b}	29.2 ± 2.4^{a}	51.5 ± 7.8^{ab}	48.7 ± 3.9^{ab}

Table 1 (*continued*)

	Date	Soil depth	Site S_9	S_{83}	S_{240}	S_{387}
	August 12th	0–5 cm	46.5 ± 8.6^{b}	33.9 ± 2.3^{ab}	42.5 ± 5.6^{b}	25.4 ± 4.8^{a}
		5–10 cm	34.8 ± 9.5	27.1 ± 3.2	38.9 ± 5.5	38.0 ± 3.7
Total C-$\delta^{13}C$ (‰)[§]		0–5 cm	−27.5 ± 0.1^{ab}	−27.8 ± 0.1^{a}	−27.1 ± 0.2^{b}	−28.2 ± 0.2^{a}
		5–10 cm	−26.5 ± 0.1^{a}	−26.3 ± 0.1^{ab}	−26.0 ± 0.1^{b}	−26.7 ± 0.1^{a}
Total N-$\delta^{15}N$ (‰)[§]		0–5 cm	−0.20 ± 0.26^{c}	−0.37 ± 0.32^{c}	−2.42 ± 0.30^{b}	−4.81 ± 0.40^{a}
		5–10 cm	1.43 ± 0.23^{b}	2.74 ± 0.14^{c}	−0.03 ± 0.31^{a}	−0.32 ± 0.25^{a}

Numbers show mean (±standard error) of replicates (n = 6). Lowercase letters indicate significant differences between the sites at each soil depth ($p < 0.05$).
[§] Mean values across two sampling dates at each depth.

acidic (pH < 6.6; Table 1). Soil pH at 5–10 cm depth on July 27th and at 0–5 cm depth on August 12th was on average 0.25 and 0.26 unit higher at the S_9 site than the S_{387} site, respectively ($p < 0.05$; Table 1).

The S_{240} site showed the highest $\delta^{13}C$ values at both soil depths, which were significantly higher than those of the S_{387} site (Table 1). All sites showed significantly different $\delta^{15}N$ values from one another ($p < 0.05$), with the exception of S_9 and S_{83} (the two low elevation sites) and S_{240} and S_{387} (the two high elevation sites), which had similar $\delta^{15}N$ values at depths of 0–5 cm and 5–10 cm, respectively (Table 1).

3.3. Carbon dioxide fluxes

Net ecosystem exchange (NEE) rates at the four sites were generally negative, indicating net atmospheric CO_2 uptake by the ecosystems (Fig. 3a). Overall, the lowest elevation site (S_9) was the largest CO_2 sink, with an average NEE rate of −197.1 mg CO_2 $m^{-2}h^{-1}$ across campaigns, while the highest elevation site (S_{387}) was the smallest CO_2 sink (on average −20.4 mg CO_2 $m^{-2}h^{-1}$; Fig. 3a). Significant higher CO_2 uptake rates were observed at the S_9 site compared with the S_{387} site during each campaign (except the 3rd campaign; $p < 0.05$; Fig. 3a).

Ecosystem respiration (ER) varied significantly between the four sites. During the 1st campaign 2-fold higher rates were observed at the S_9 site compared with the S_{240} site ($p < 0.007$), and during the 3rd campaign the S_{387} site showed 2-fold higher rates than the S_{83} site ($p = 0.0027$; Fig. 3b). On the 3rd and 4th campaigns, ER rates were significantly higher at the S_9 site than the other three sites ($p < 0.05$; Fig. 3b).

Gross ecosystem photosynthesis (GEP) rates ranged from −611.4 to −182.2 mg CO_2 m^{-2} h^{-1} among the four sites, with the highest photosynthetic activity at the S_9 site (on average −522.9 mg CO_2 m^{-2} h^{-1}; Fig. 3c). The S_9 site had about 2-fold higher photosynthetic activity than the other three sites on the 3rd and 4th campaigns ($p < 0.01$; Fig. 3c).

3.4. PAR and NDVI

Significantly different incoming PAR values were measured between the four campaigns for the S_9 and S_{83} sites ($p < 0.01$; Fig. S3a). For the S_{240} and S_{387} sites, PAR at the first three campaigns were significantly higher than the last one ($p < 0.05$; Fig. S3a). In addition, at the S_{387} site, the first campaign showed significantly higher PAR than the second campaign ($p < 0.01$; Fig. S3a).

Over the measurement period, a tendency for a decreasing NDVI with time was observed (Fig. S3b). The S_9 and S_{387} sites had higher NDVI values than the other two sites during the whole study period ($p < 0.05$), although at the last campaigns the S_9 site did not significantly differ from the S_{240} site (Fig. S3b).

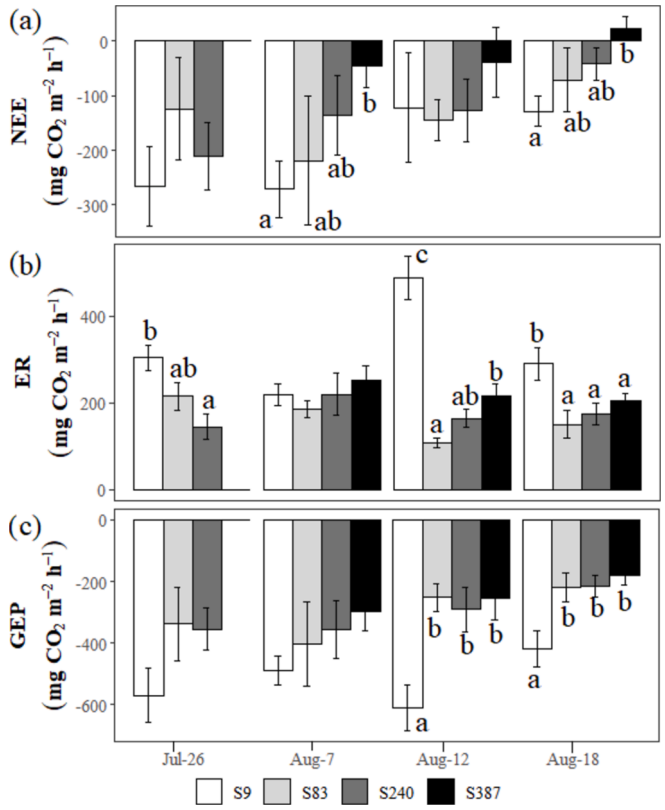

Fig. 3. Net ecosystem exchange (NEE) (a), ecosystem respiration (ER) (b), and gross ecosystem production (GEP) (c) rates from the four study sites in Disko Island, West Greenland. Bars show mean of replicates (n = 6). Error bars are standard error. Lowercase letters indicate significant differences between the sites on each measurement day ($p < 0.05$).

3.5. Temperature and moisture response

Soil respiration across sites increased from 0.5 to 92.4 mg CO_2 m^{-2} h^{-1} with incubation temperatures increasing from −10 to 15 °C (Fig. S4). The Q_{10} values for the soil respiration measurements both above and below 0 °C, and relationship between soil respiration and incubation temperatures are shown in Figs. 4 and S5. The soil respiration overall showed much higher Q_{10} values for the temperature below 0 °C, up to 25 times the ones above 0 °C (Fig. 4). The highest elevation site (S_{387}) had the highest Q_{10} values for the temperature above 0 °C, but not different from S_{83} and S_{240}, while below 0 °C the S_{240} site showed the highest Q_{10} values though not different from S_9 and S_{387} (Fig. 4). For the measurements above 0 °C Q_{10} values were significantly higher at the highest site (S_{387}) than the lowest site (S_9, $p = 0.05$), whereas for the measurements below 0 °C the S_{240} site had 2-fold higher Q_{10} values than the S_{83} site ($p = 0.05$; Fig. 4).

In general, a maximum of normalized soil respiration was observed between 35 % and 45 % WFPS at all the four sites (Figs. S6 and S7). The lowest moisture sensitivity of soil respiration was observed at the S_{83} site, while the lowest (S_9) and highest sites (S_{387}) had the highest values (Fig. 4c), yet not significantly different among sites.

3.6. Correlations between CO_2 fluxes and Q_{10} values, and NDVI and soil properties

The stepwise regression analysis showed that the NEE rates across sites were explained by soil moisture ($R^2 = 0.119$), the GEP rates were equally explained by soil temperature and soil moisture (with their relative importance of 49.1 % and 50.8 %, respectively; $R^2 = 0.196$), and the ER rates were explained by NDVI and soil temperature (with their relative importance of 60.0 % and 39.9 %, respectively; $R^2 = 0.191$; Table 2).

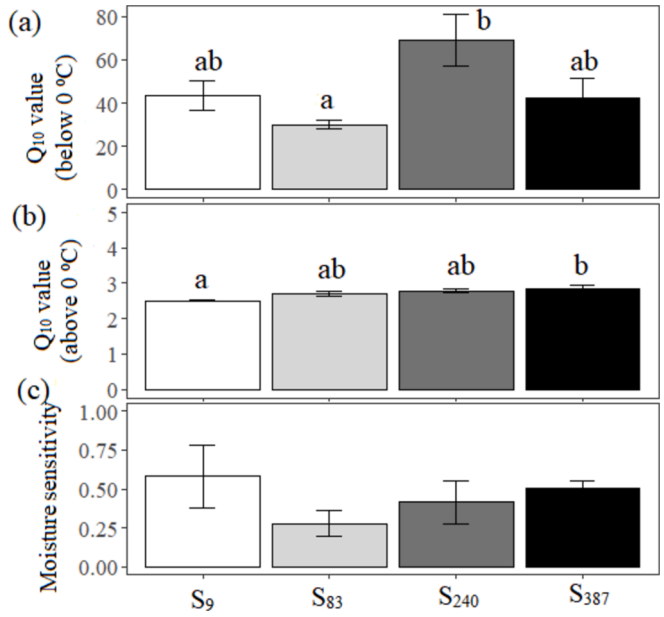

Fig. 4. The Q_{10} values at temperatures below 0 °C (a), Q_{10} values at temperatures above 0 °C (b), and moisture sensitivity of soil respiration (c) from the four study sites in Disko Island, West Greenland. Bars show mean of replicates (n = 6). Error bars are standard error. Lowercase letters indicate significant differences between the sites ($p < 0.05$).

According to Pearson correlation analysis, the Q_{10} values for the temperature above 0 °C were significantly and positively correlated with soil C: N ratios, while the Q_{10} values for the temperature below 0 °C were positively related to soil NH_4^+-N concentrations, total soil C and N contents, and soil temperature (Fig. 5).

Principal component analysis (PCA) was used to determine the clustering of all variables among the study sites (Fig. 6). The lowest (S_9) and highest (S_{387}) elevation sites separated from each other, while they both appeared to cluster with the intermediate elevation sites (Fig. 6). The S_9 site was associated with high soil moisture, soil pH, and air temperature, and the S_{387} site was related with Q_{10} values (above 0 °C) and soil C:N ratio (Fig. 6).

4. Discussion

4.1. Air temperature and soil nutrient status

According to the dry adiabatic lapse rate, 100 m upward can cause a temperature drop of 0.98 °C. In this study, an increase of 1.8 °C in mean daily air temperature from the S_{83} site to the S_{240} site and a fall of 0.2 °C from the S_{240} site to the S_{387} site were observed during the study period. This pattern of the temperature variation between the sites is in

Table 2
Multiple stepwise regression analysis of the relationship between NEE, ER and GEP, and soil temperature, soil moisture, NDVI and PAR (n = 90).

Response variable	Predictor variable	Relative importance of the variable (%)	P value	Proportion of variance explained by model (%)
NEE	Soil moisture		0.001	11.9
ER	Soil temperature	39.9	0.001	19.6
	NDVI	60.0	0.016	
GEP	Soil temperature	49.1	0.006	19.1
	Soil moisture	50.8	0.005	

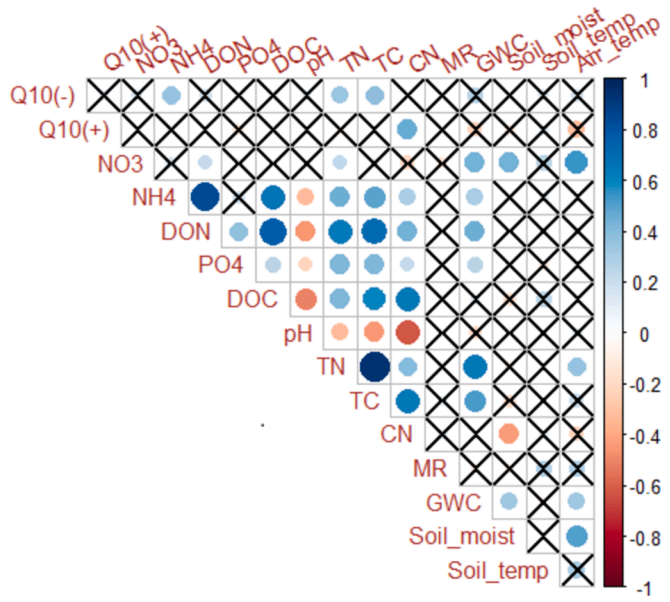

Fig. 5. Pearson correlation analysis between Q_{10} values, moisture sensitivity, site elevations and soil physicochemical properties across the study sites (n = 24). Q_{10} (−): Q_{10} values below 0 °C, Q_{10} (+): Q_{10} values above 0 °C, NO3: soil NO_3^--N, NH4: soil NH_4^+-N, DON: soil dissolved organic N, PO4: soil PO_4^{3+}-P, DOC: soil dissolved organic C, TN: soil total N, TC: soil total C, CN: soil C:N ratio, MR: moisture sensitivity of soil respiration, GWC: gravimetric water content, Soil_moist: soil moisture content, Soil_temp: soil temperature, Air_temp: air temperature. The colors indicate positive or negative correlations and the size of circles signifies the strength of the correlations. Non-significant correlations ($p > 0.05$) are marked with ×.

accordance with the long-term air temperature data (Fig. 2). This supports that the development of temperature inversion layers is prominent in the area, in agreement with a more regional perspective by e.g. Shahi et al. (2023). Hence, the direction and magnitude of changes in air temperatures along the elevation gradient is not consistent, while topographic differences may affect microclimate at the sites. The rise in air temperature from the S_{83} site to the sites of higher elevation may be explained by differences in the wind exposure. The S_{83} site is clearly more exposed to winds, as it is situated on more open terrain, while the other sites are more protected from the winds. McIntire et al. (2016) found that wind exposure rather than elevation played a major role in controlling air temperature across different mountain regions on three continents. Soil temperatures neither varied along the elevation gradient, nor followed the same patterns as the air temperature for the sites likely because soil temperature additionally is influenced by solar radiation, vegetation cover and hydrological conditions (Aalto et al., 2013; Ni et al., 2019).

The soil organic matter, as indicated by the total C content, did not differ among the four study sites. This suggests that net accumulation of SOM occurs at comparable rates along the elevational gradient. Site differences in soil nutrient availability did not follow a consistent pattern with elevation. In general, the coolest site (S_{83}) had the poorest soil nutrient status, suggesting that temperature is a key limiting factor for soil processes in arctic tundra ecosystems. However, the low soil N nutrient status at the low elevation site might be a result of large gaseous losses. Soil microbial processes such as nitrification and denitrification discriminate against ^{15}N, likely resulting in losses of ^{15}N-depleted N forms from soils via N_2O/N_2 emissions and leaving the remaining soil N fraction progressively ^{15}N-enriched (Pörtl et al., 2007). This is supported by the high bulk soil $\delta^{15}N$ at the S_{83} site. The highest NH_4^+-N concentrations at both soil depths were generally observed at the highest elevation site, which was likely attributed to high soil temperatures and dissolved organic N availability, and thus fast N mineralization. Meanwhile, nitrification and soil NO_3^--N concentrations were shown to linearly correlate with the amount of NH_4^+ supplied by mineralization (Turner et al., 2007; Frerichs et al., 2020). However, this does not appear to be the case for our study sites. The highest elevation site exhibited low soil NO_3^--N concentrations at both depths despite the highest soil NH_4^+-N

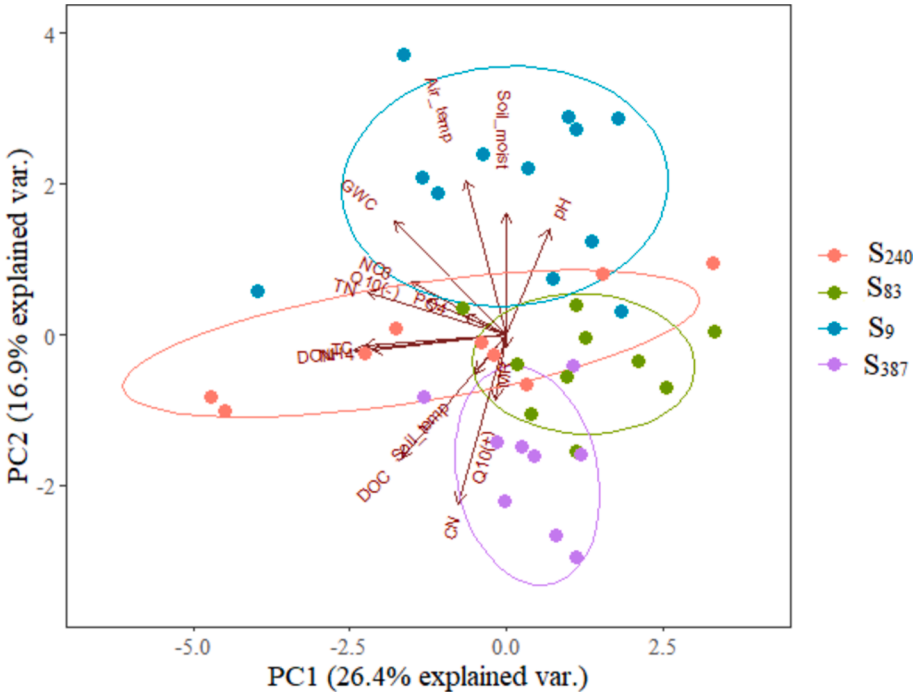

Fig. 6. Principal component analysis (PCA) for Q_{10} values, moisture sensitivity, site elevations and soil physicochemical properties across the study sites (n = 43). The S9 site have 12 points, while the other sites have 10–11 points due to missing replicate values. Q_{10} (−): Q_{10} values below 0 °C, Q_{10} (+): Q_{10} values above 0 °C, NO_3: soil NO_3^--N, NH_4: soil NH_4^+-N, DON: soil dissolved organic N, PO_4: soil PO_4^{3+}-P, DOC: soil dissolved organic C, TN: soil total N, TC: soil total C, CN: soil C/N ratio, MR: moisture sensitivity of soil respiration, GWC: gravimetric water content, Soil_moist: soil moisture content, Soil_temp: soil temperature, Air_temp: air temperature.

concentrations. We speculate that this is because plant and microbial assimilation may outcompete NH_4^+ uptake by nitrifiers (Turner et al., 2007; Tsui and Chen, 2010), given that N is one of the most limiting nutrients in tundra ecosystems (Xu et al., 2021b; Xu et al., 2023). In addition, soil organic matter composition may impact the balance between NH_4^+ acquisition by heterotrophs and nitrifiers (Booth et al., 2005; Dan et al., 2022). Nitrification and NH_4^+ loss have been found to vary inversely with soil C:N ratios, suggesting that increasing soil C:N ratios may promote NH_4^+ assimilation or suppress NO_3^- production (Corre et al., 2007; Celi et al., 2022). The redistribution of soluble nutrients with water and snow when moving from upland to low-lying areas could be another explanation (Paré and Bedard-Haughn, 2012; Christiansen et al., 2017). Nitrate is very mobile and loosely bound in the soil and hence easily leached (Borchard et al., 2019), likely leading to the low soil NO_3^--N concentrations at the highest elevation site. The lowest elevation site generally showed the highest soil mineral N concentrations at both depths, which could be due to the combined effects of favorable soil microclimate and nutrient movement. According to the PCA analysis, the four study sites appeared to cluster with each other, except that the lowest (S_9) and highest (S_{387}) elevation sites separated. This suggests that the characteristics (e.g., soil nutrient status and soil microclimate conditions) of the study sites could not be solely differentiated by the elevation, at least for the sites lacking marked differences in elevation.

4.2. Ecosystem-atmosphere CO_2 exchange

The magnitude of measured NEE (ranging from −266.1 to 23.0 mg CO_2 m^{-2} h^{-1}) and GEP rates (from −611.4 to −182.2 mg CO_2 m^{-2} h^{-1}) among four study sites were comparable with the flux rates reported in Zackenberg, Northest Greenland (Christensen et al., 2000; Pirk et al., 2016) and Disko, West Greenland (Ravn et al., 2020). The ER was slightly larger than has been found at Disko dry tundra (Ravn et al., 2020), likely because our observations captured a limited, warm period in July-August, providing a snapshot of that specific timeframe. But it was well within the range of the values reported in other arctic sites (Dagg and Lafleur, 2011; Treharne et al., 2019).

Since no consistent temperature gradient was found along the elevation gradient, the elevation and its anticipated effect on temperature and soil nutrients were not the factors influencing the surface CO_2 fluxes in this area. This leads to rejection of our hypotheses (H1) and (H2) that air and soil temperatures and soil nutrients as well as ecosystem CO_2 exchange rates decrease with increasing elevation. But topography aspect-induced soil microclimate differences were observed to affect the surface CO_2 fluxes. According to the regression analysis, soil temperatures and NDVI were two factors influencing the ER rates across the study sites. It is well-known that soil temperature is a constraint on soil microbial respiration in the Arctic (Hartley et al., 2008; Sullivan et al., 2020). Soil temperature can also alter plant growth by influencing water and nutrient uptake as well as root and shoot growth (Heinze et al., 2017; Onwuka and Mang, 2018), leading to an impact on both above-ground plant and root respiration. A more productive canopy with higher leaf area (assessed by NDVI) has higher above-ground plant respiration (Parker et al., 2015), and may also supply more rhizosphere C and accelerate root and soil microbial respiration (Parker et al., 2020; Azevedo et al., 2021). The variations of GEP rates among the study sites were driven by soil temperatures and soil moisture. The GEP rates in tundra ecosystems have been reported to be strongly linked with soil temperatures and soil moisture at both plot and landscape levels (Dagg and Lafleur, 2011; Virkkala et al., 2018). High soil temperatures and moisture can directly increase plant photosynthetic rates and thus promote ecosystem C assimilation (Starr et al., 2008; Göbel et al., 2019). High soil temperatures and moisture may also promote soil nutrient availability and plant mineral nutrition, growth and productivity, indirectly enhancing plant photosynthetic capacity (Welker et al., 2004; Ramm et al., 2022). This is reflected by the highest photosynthetic activity at the lowest elevation site that had the highest soil mineral N concentrations. However, the GEP rates were not found to vary with NDVI, which was attributed to the fact that S_{387} and S_9 sites had similar high NDVI, but contrasting GEP rates. It's plausible that NDVI, used as a proxy for vegetation productivity, may not fully capture all relevant factors influencing GEP. Spatial heterogeneity within the study area, including variations in soil properties and microclimate conditions could contribute to differences in GEP that are not reflected in NDVI measurements.

Although our stepwise regression analysis shows the main explanatory variables for surface CO_2 fluxes, the relatively low proportion of explained variance implies the influence of additional factors (e.g., microbial activity and root respiration) not captured in the model (Hopkins et al., 2013). Furthermore, our limitation of using a small sample size in regression analysis could lead to biased estimates and limited generalizability of results. With a small number of samples, the variability within the data may not be adequately represented, leading to imprecise parameter estimates. The generalizability of findings from analyses with small sample sizes may be limited to the specific conditions from which the samples were drawn, making it challenging to extrapolate the results to broader contexts.

4.3. Temperature and moisture sensitivity of soil respiration

Soil respiration activities were observed down to −10 °C, consistent with the observations by Elberling and Brandt (2003) of respiration down to −15 °C in soils from high arctic Zackenberg, NE Greenland. An exponential rise of soil respiration (below 0 °C) was found with increasing temperature at the four study sites. The high Q_{10} values at temperatures below 0 °C were comparable with the Q_{10} of 21.7 (below 0 °C) reported at Nødebo, Denmark and Q_{10} of 50.8 (below 0 °C) reported at Zackenberg, Greenland (Elberling and Brandt, 2003). This is likely because most of the produced CO_2 was trapped in frozen soil and abruptly released around 0 °C (Elberling and Brandt, 2003). The unfrozen water content of soils below 0 °C may also control the temperature response of respiration by altering the diffusions of substrates, nutrients, and waste products, and the extent of intracellular dehydration. Since neither soil volumetric moisture (*in-situ*) and nor soil gravimetric water content was linked to Q_{10} values, we speculate that the contrasting soil water status among the four study sites did not affect the unfrozen water content when soils froze. The Q_{10} values (below 0 °C) were significantly correlated with soil NH_4^+-N, and total C and N contents across the study sites. As soils freeze, microbial substrate use shifts from detrital material to dead microbial biomass, products of microbial metabolism, and labile organic compounds (Mikan et al., 2002; Sullivan et al., 2020). The quantity of these substrates (as indicated by total C and N contents) could largely influence soil microbial respiration below 0 °C. In the arctic tundra, soil microbes are able to assimilate NH_4^+-N for the synthesis of proteins and other labile organic N compounds during winter (below 0 °C) (Schimel et al., 2004; Xu et al., 2021b). Since active microbes are limited to thin water films when soils freeze, they rely extensively on the organic substrates from recycling of microbial necromass and small labile compounds that may remain in water films (Schimel and Mikan, 2005; Schaefer and Jafarov, 2016). High availability of NH_4^+-N appears to promote microbial N assimilation and in turn provides more microbial-derived compounds that are easily accessible for microbes under frozen conditions (Makarov et al., 2008). Thus, soil NH_4^+-N availability was also a key factor in controlling the temperature response of soil microbial respiration (below 0 °C).

Above 0 °C an increasing Q_{10} value was found with increasing elevation, which indicates that soil respiration at the higher elevation sites were more affected by a rise in temperature than the lower sites. A relationship between Q_{10} and mean annual air temperature or soil temperature along elevation gradients has been reported in various ecosystems, and the larger Q_{10} values at the higher elevations were due to their colder temperatures (Schindlbacher et al., 2010; Gutiérrez-Girón

et al., 2015; Nottingham et al., 2016; Nottingham et al., 2019). However, in the current study, no apparent temperature gradient was observed, and hence the variations of Q_{10} (above 0 °C) cannot be explained by the temperature differences. The snow cover depth and duration have been found to increase with elevation in this study area (Pedersen et al., 2016). The high elevation sites exhibited correspondingly high Q_{10} values (above 0 °C), which could be attributed to the increasing snow cover duration. The longer snow cover duration shortens the growing season (available for plant growth) and changes the ratio between the input of fresh organic matter and the microbial decomposition rates, and thus the decomposition process becomes more dependent on temperature (Ohkubo et al., 2012; Bracho et al., 2016). There were also significant correlations between Q_{10} values and soil C:N ratios among the study sites. Generally, soil C:N ratio is an indicator of the recalcitrant fractions of carbonyl and aromatic C, and the ratio of recalcitrant C to labile C (Soong and Cotrufo, 2015; Zhang et al., 2019). According to the basic thermodynamic theory, enzymatic reactions metabolizing structurally complex, aromatic C molecules have higher activation energies and temperature dependence than reactions metabolizing structurally simpler C molecules (Billings and Ballantyne, 2013; Pradel et al., 2023). For example, Xu et al. (2010) found temperature response of soil respiration to increase with soil organic C recalcitrance along an elevation gradient in the mountains. All the four study sites showed much higher Q_{10} values below than above 0 °C. This again suggests that the low amount of liquid water in soils below freezing point has restricted substrate diffusion and microbial activity and thereby soil respiration (Öquist et al., 2009; Schaefer and Jafarov, 2016).

The optimum water content for soil respiration is frequently found at intermediate values (Balogh et al., 2011), where the macropores were mostly air filled, hence facilitating O_2 diffusion, and the micropores were mostly water filled facilitating substrate diffusion (Zhang et al., 2015). Consistent with previous studies (Sun et al., 2018; Xu et al., 2021a; Azizi-Rad et al., 2022), our incubation experiment showed that the maximum soil respiration was at 35–45 % WFPS for all the study sites. Soil respiration in the lowest (S_9, wettest) and highest (S_{387}, driest) elevation sites was more sensitive to the increase in water content compared with the other two sites. This is partly consistent with the observations by Azizi-Rad et al. (2022) that moisture sensitivity of decomposition in soils from a Tibetan grassland was higher under both nearly dry and saturated conditions, because more energy was required for microbial activity under those conditions. At our driest site a low soil water content could constrain the diffusion of substrates, extracellular enzymes, and microbial mobility, while at the wettest site high soil water content may slow the diffusion of O_2. Thus, soil microbial respiration in these two sites seemed to be inhibited by their moisture conditions and became more responsive to the changes in soil water content.

Overall, our results showed increasing temperature sensitivity (above 0 °C) but no clear patterns of temperature (below 0 °C) and moisture sensitivity of soil respiration with increasing elevation, partly supporting hypothesis H3. However, our small sample sizes are more susceptible to outliers and influential data points, which could distort the estimated relationships between variables (soil respiration vs. temperatures) and undermine the validity of the findings.

5. Conclusion

This study addresses the knowledge gap regarding how ecosystem CO_2 exchange and temperature and moisture sensitivity of soil respiration vary along an elevation gradient in an arctic tundra ecosystem. No apparent temperature gradient was found along the elevation gradient, and thus the elevation was not the factor affecting the soil nutrient status in this area. The absolute differences in CO_2 fluxes among the sites were significant, while the elevation was not the factor influencing ecosystem CO_2 exchange. Rather topography aspect-induced soil microclimate differences were the primary drivers for the ecosystem CO_2 exchange, possibly amplified by local-scale temperature inversions layers. However, expanding the sampling framework to include long-term CO_2 measurements at multiple heights within the ecosystem is necessary to comprehensively assess spatial and temporal variability and to understand the drivers of differences in fluxes. Although the temperature sensitivity of soil respiration above 0 °C increased with increasing elevation, whereas the temperature sensitivity below 0 °C and the moisture sensitivity were not regulated by the elevation but by soil N availability. Elevation is an important factor to consider when upscaling to regional CO_2 fluxes particularly during growing seasons and predicting how tundra ecosystems at different elevations will respond to climate change. However, other factors such as soil nutrient availability and microclimate conditions are likely to be more influential in driving the variations in ecosystem CO_2 fluxes during winter (under sub-zero conditions). Ecosystem models should be modified and parameterized accordingly to reflect the importance of these other factors and their interactions to accurately predict CO_2 fluxes in the arctic tundra region.

CRediT authorship contribution statement

Wenyi Xu: Data curation, Formal analysis, Visualization, Writing – original draft, Writing – review & editing. **Andreas Westergaard-Nielsen:** Investigation, Supervision, Writing – review & editing. **Anders Michelsen:** Resources, Writing – review & editing. **Per Lennart Ambus:** Conceptualization, Data curation, Funding acquisition, Investigation, Methodology, Project administration, Supervision, Writing – review & editing.

Declaration of competing interest

The authors declare that they have no known competing financial interests or personal relationships that could have appeared to influence the work reported in this paper.

Acknowledgements

We gratefully acknowledge the financial support from the Danish National Research Foundation (CENPERM DNRF100). We extend our gratitude to Arctic Station for their collaboration and logistical support during the fieldwork, and to MSc. Malene Bille Nielsen for her invaluable assistance with field- and laboratory work and data analyses. We would like to thank Yijing Liu (University of Copenhagen) for snow depth modelling, although these data were not included.

Appendix A. Supplementary data

Supplementary data to this article can be found online at https://doi.org/10.1016/j.geoderma.2024.117108.

Data availability

Data will be made available on request.

References

Aalto, J., le Roux, P.C., Luoto, M., 2013. Vegetation mediates soil temperature and moisture in arctic-alpine environments. Arct. Antarct. Alp. Res. 45, 429–439.
Azevedo, O., Parker, T.C., Siewert, M.B., Subke, J.-A., 2021. Predicting soil respiration from plant productivity (NDVI) in a sub-Arctic tundra ecosystem. Remote Sens. (Basel) 13, 2571.
Azizi-Rad, M., Guggenberger, G., Ma, Y., Sierra, C.A., 2022. Sensitivity of soil respiration rate with respect to temperature, moisture and oxygen under freezing and thawing. Soil Biol. Biochem. 165, 108488.
Balogh, J., Pintér, K., Fóti, S., Cserhalmi, D., Papp, M., Nagy, Z., 2011. Dependence of soil respiration on soil moisture, clay content, soil organic matter, and CO_2 uptake in dry grasslands. Soil Biol. Biochem. 43, 1006–1013.
Bauer, J., Weihermüller, L., Huisman, J., Herbst, M., Graf, A., Sequaris, J., Vereecken, H., 2012. Inverse determination of heterotrophic soil respiration response to

temperature and water content under field conditions. Biogeochemistry 108, 119–134.
Billings, S.A., Ballantyne IV, F., 2013. How interactions between microbial resource demands, soil organic matter stoichiometry, and substrate reactivity determine the direction and magnitude of soil respiratory responses to warming. Glob. Chang. Biol. 19, 90–102.
Boddy, E., Roberts, P., Hill, P.W., Farrar, J., Jones, D.L., 2008. Turnover of low molecular weight dissolved organic C (DOC) and microbial C exhibit different temperature sensitivities in Arctic tundra soils. Soil Biol. Biochem. 40, 1557–1566.
Booth, M.S., Stark, J.M., Rastetter, E., 2005. Controls on nitrogen cycling in terrestrial ecosystems: a synthetic analysis of literature data. Ecol. Monogr. 75, 139–157.
Borchard, N., Schirrmann, M., Cayuela, M.L., Kammann, C., Wrage-Mönnig, N., Estavillo, J.M., Fuertes-Mendizábal, T., Sigua, G., Spokas, K., Ippolito, J.A., 2019. Biochar, soil and land-use interactions that reduce nitrate leaching and N_2O emissions: a meta-analysis. Sci. Total Environ. 651, 2354–2364.
Bracho, R., Natali, S., Pegoraro, E., Crummer, K.G., Schädel, C., Celis, G., Hale, L., Wu, L., Yin, H., Tiedje, J.M., 2016. Temperature sensitivity of organic matter decomposition of permafrost-region soils during laboratory incubations. Soil Biol. Biochem. 97, 1–14.
Carey, J.C., Tang, J., Templer, P.H., Kroeger, K.D., Crowther, T.W., Burton, A.J., Dukes, J.S., Emmett, B., Frey, S.D., Heskel, M.A., 2016. Temperature response of soil respiration largely unaltered with experimental warming. Proc. Natl. Acad. Sci. 113, 13797–13802.
Celi, L., Said-Pullicino, D., Bol, R., Lang, F., Luster, J., 2022. Interconnecting soil organic matter with nitrogen and phosphorus cycling. Multi-Scale Biogeochemical Processes in Soil Ecosystems: Critical Reactions and Resilience to Climate Changes, 51–77.
Christensen, T.R., Friborg, T., Sommerkorn, M., Kaplan, J., Illeris, L., Soegaard, H., Nordstroem, C., Jonasson, S., 2000. Trace gas exchange in a high-Arctic valley: 1. Variationsin CO_2 and CH_4 flux between tundra vegetation types. Global Biogeochem. Cycles 14, 701–713.
Christiansen, C.T., Haugwitz, M.S., Priemé, A., Nielsen, C.S., Elberling, B., Michelsen, A., Grogan, P., Blok, D., 2017. Enhanced summer warming reduces fungal decomposer diversity and litter mass loss more strongly in dry than in wet tundra. Glob. Chang. Biol. 23, 406–420.
Córdova, M., Célleri, R., Shellito, C.J., Orellana-Alvear, J., Abril, A., Carrillo-Rojas, G., 2016. Near-surface air temperature lapse rate over complex terrain in the Southern Ecuadorian Andes: implications for temperature mapping. Arct. Antarct. Alp. Res. 48, 673–684.
Corre, M.D., Brumme, R., Veldkamp, E., Beese, F.O., 2007. Changes in nitrogen cycling and retention processes in soils under spruce forests along a nitrogen enrichment gradient in Germany. Glob. Chang. Biol. 13, 1509–1527.
Dagg, J., Lafleur, P., 2011. Vegetation community, foliar nitrogen, and temperature effects on tundra CO_2 exchange across a soil moisture gradient. Arct. Antarct. Alp. Res. 43, 189–197.
Dan, X., Meng, L., He, M., He, X., Zhao, C., Chen, S., Zhang, J., Cai, Z., Müller, C., 2022. Regulation of nitrogen acquisition in vegetables by different impacts on autotrophic and heterotrophic nitrification. Plant Soil 474, 581–594.
Dan, W., Nianpeng, H., Qing, W., Yuliang, L., Qiufeng, W., Zhiwei, X., Jianxing, Z., 2016. Effects of temperature and moisture on soil organic matter decomposition along elevation gradients on the Changbai Mountains, Northeast China. Pedosphere 26, 399–407.
Davidson, E.A., Janssens, I.A., Luo, Y., 2006. On the variability of respiration in terrestrial ecosystems: moving beyond Q10. Glob. Chang. Biol. 12, 154–164.
Elberling, B., 2007. Annual soil CO_2 effluxes in the High Arctic: the role of snow thickness and vegetation type. Soil Biol. Biochem. 39, 646–654.
Elberling, B., Brandt, K.K., 2003. Uncoupling of microbial CO_2 production and release in frozen soil and its implications for field studies of arctic C cycling. Soil Biol. Biochem. 35, 263–272.
Findlay, H.S., Gibson, G., Kędra, M., Morata, N., Orchowska, M., Pavlov, A.K., Reigstad, M., Silyakova, A., Tremblay, J.-E., Walczowski, W., 2015. Responses in Arctic marine carbon cycle processes: conceptual scenarios and implications for ecosystem function. Polar Res. 34, 24252.
Flerchinger, G.N., Fellows, A.W., Seyfried, M.S., Clark, P.E., Lohse, K.A., 2020. Water and carbon fluxes along an elevational gradient in a sagebrush ecosystem. Ecosystems 23, 246–263.
Frerichs, C., Daum, D., Pacholski, A.S., 2020. Ammonia and ammonium exposure of basil (Ocimum basilicum L.) growing in an organically fertilized peat substrate and strategies to mitigate related harmful impacts on plant growth. Front. Plant Sci. 10, 1696.
Garten Jr, C.T., Hanson, P.J., 2006. Measured forest soil C stocks and estimated turnover times along an elevation gradient. Geoderma 136, 342–352.
Göbel, L., Coners, H., Hertel, D., Willinghöfer, S., Leuschner, C., 2019. The role of low soil temperature for photosynthesis and stomatal conductance of three graminoids from different elevations. Front. Plant Sci. 10, 330.
Gutiérrez-Girón, A., Díaz-Pinés, E., Rubio, A., Gavilán, R.G., 2015. Both altitude and vegetation affect temperature sensitivity of soil organic matter decomposition in Mediterranean high mountain soils. Geoderma 237, 1–8.
Hartley, I.P., Hopkins, D.W., Garnett, M.H., Sommerkorn, M., Wookey, P.A., 2008. Soil microbial respiration in arctic soil does not acclimate to temperature. Ecol. Lett. 11, 1092–1100.
Heijmans, M.M., Magnússon, R.Í., Lara, M.J., Frost, G.V., Myers-Smith, I.H., van Huissteden, J., Jorgenson, M.T., Fedorov, A.N., Epstein, H.E., Lawrence, D.M., 2022. Tundra vegetation change and impacts on permafrost. Nat. Rev. Earth Environ. 3, 68–84.
Heinze, J., Gensch, S., Weber, E., Joshi, J., 2017. Soil temperature modifies effects of soil biota on plant growth. J. Plant Ecol. 10, 808–821.
Hopkins, F., Gonzalez-Meler, M.A., Flower, C.E., Lynch, D.J., Czimczik, C., Tang, J., Subke, J.A., 2013. Ecosystem-level controls on root-rhizosphere respiration. New Phytol. 199, 339–351.
Karhu, K., Auffret, M.D., Dungait, J.A., Hopkins, D.W., Prosser, J.I., Singh, B.K., Subke, J.-A., Wookey, P.A., Ågren, G.I., Sebastia, M.-T., 2014. Temperature sensitivity of soil respiration rates enhanced by microbial community response. Nature 513, 81–84.
Kim, Y., Kim, S.-D., Enomoto, H., Kushida, K., Kondoh, M., Uchida, M., 2013. Latitudinal distribution of soil CO_2 efflux and temperature along the Dalton Highway. Alaska Polar Sci. 7, 162–173.
Knowles, J.F., Blanken, P.D., Williams, M.W., 2015. Soil respiration variability across a soil moisture and vegetation community gradient within a snow-scoured alpine meadow. Biogeochemistry 125, 185–202.
Kobayashi, H., Yunus, A.P., Nagai, S., Sugiura, K., Kim, Y., Van Dam, B., Nagano, H., Zona, D., Harazono, Y., Bret-Harte, M.S., 2016. Latitudinal gradient of spruce forest understory and tundra phenology in Alaska as observed from satellite and ground-based data. Remote Sens. Environ. 177, 160–170.
Körner, C., 2021. The climate plants experience. Alpine Plant Life: functional plant ecology of high mountain ecosystems, 65–88.
Lenth, R., 2020. Emmeans: estimated marginal means, aka least-squares means. Rpackage version 1.4. 7. 2020.
Ma, M., Zang, Z., Xie, Z., Chen, Q., Xu, W., Zhao, C., Shen, G., 2019. Soil respiration of four forests along elevation gradient in northern subtropical China. Ecol. Evol. 9, 12846–12857.
Makarov, M., Malysheva, T., Cornelissen, J., van Logtestijn, R., Glasser, B., 2008. Consistent patterns of 15N distribution through soil profiles in diverse alpine and tundra ecosystems. Soil Biol. Biochem. 40, 1082–1089.
Mankin, E., 2008. Principal components analysis: a how-to manual for R. Desde http://psych.colorado.edu/wiki/lib/exe/fetch.php.
McIntire, E.J., Piper, F.I., Fajardo, A., 2016. Wind exposure and light exposure, more than elevation-related temperature, limit tree line seedling abundance on three continents. J. Ecol. 104, 1379–1390.
Mikan, C.J., Schimel, J.P., Doyle, A.P., 2002. Temperature controls of microbial respiration in arctic tundra soils above and below freezing. Soil Biol. Biochem. 34, 1785–1795.
Morgner, E., Elberling, B., Strebel, D., Cooper, E.J., 2010. The importance of winter in annual ecosystem respiration in the High Arctic: effects of snow depth in two vegetation types. Polar Res. 29, 58–74.
Moyano, F.E., Manzoni, S., Chenu, C., 2013. Responses of soil heterotrophic respiration to moisture availability: an exploration of processes and models. Soil Biol. Biochem. 59, 72–85.
Ni, J., Cheng, Y., Wang, Q., Ng, C.W.W., Garg, A., 2019. Effects of vegetation on soil temperature and water content: field monitoring and numerical modelling. J. Hydrol. 571, 494–502.
Nottingham, A.T., Turner, B.L., Whitaker, J., Ostle, N., Bardgett, R.D., McNamara, N.P., Salinas, N., Meir, P., 2016. Temperature sensitivity of soil enzymes along an elevation gradient in the Peruvian Andes. Biogeochemistry 127, 217–230.
Nottingham, A.T., Bååth, E., Reischke, S., Salinas, N., Meir, P., 2019. Adaptation of soil microbial growth to temperature: using a tropical elevation gradient to predict future changes. Glob. Chang. Biol. 25, 827–838.
Oberbauer, S.F., Tweedie, C.E., Welker, J.M., Fahnestock, J.T., Henry, G.H.R., Webber, P. J., Hollister, R.D., Walker, M.D., Kuchy, A., Elmore, E., Starr, G., 2007. Tundra CO_2 fluxes in response to experimental warming across latitudinal and moisture gradients. Ecol. Monogr. 77, 221–238.
Ohkubo, S., Iwata, Y., Hirota, T., 2012. Influence of snow-cover and soil-frost variations on continuously monitored CO_2 flux from agricultural land. Agric. For. Meteorol. 165, 25–34.
Onwuka, B., Mang, B., 2018. Effects of soil temperature on some soil properties and plant growth. Adv. Plants Agric. Res. 8, 34–37.
Öquist, M.G., Sparrman, T., Klemedtsson, L., Drotz, S.H., Grip, H., Schleucher, J., Nilsson, M., 2009. Water availability controls microbial temperature responses in frozen soil CO_2 production. Glob. Chang. Biol. 15, 2715–2722.
Panikov, N., Flanagan, P., Oechel, W., Mastepanov, M., Christensen, T., 2006. Microbial activity in soils frozen to below− 39 C. Soil Biol. Biochem. 38, 785–794.
Paré, M.C., Bedard-Haughn, A., 2012. Landscape-scale N mineralization and greenhouse gas emissions in Canadian Cryosols. Geoderma 189, 469–479.
Parker, T.C., Subke, J.A., Wookey, P.A., 2015. Rapid carbon turnover beneath shrub and tree vegetation is associated with low soil carbon stocks at a subarctic treeline. Glob. Chang. Biol. 21, 2070–2081.
Parker, T.C., Clemmensen, K.E., Friggens, N.L., Hartley, I.P., Johnson, D., Lindahl, B.D., Olofsson, J., Siewert, M.B., Street, L.E., Subke, J.A., 2020. Rhizosphere allocation by canopy-forming species dominates soil CO_2 efflux in a subarctic landscape. New Phytol. 227, 1818–1830.
Pedersen, S.H., Tamstorf, M.P., Abermann, J., Westergaard-Nielsen, A., Lund, M., Skov, K., Sigsgaard, C., Mylius, M.R., Hansen, B.U., Liston, G.E., 2016. Spatiotemporal characteristics of seasonal snow cover in Northeast Greenland from in situ observations. Arct. Antarct. Alp. Res. 48, 653–671.
Pirk, N., Tamstorf, M.P., Lund, M., Mastepanov, M., Pedersen, S.H., Mylius, M.R., Parmentier, F.J.W., Christiansen, H.H., Christensen, T.R., 2016. Snowpack fluxes of methane and carbon dioxide from high Arctic tundra. J. Geophys. Res. Biogeo. 121, 2886–2900.
Pörtl, K., Zechmeister-Boltenstern, S., Wanek, W., Ambus, P., Berger, T.W., 2007. Natural 15N abundance of soil N pools and N2O reflect the nitrogen dynamics of forest soils. Plant and Soil 295, 79–94.

Pradel, P., Bravo, L.A., Merino, C., Trefault, N., Rodríguez, R., Knicker, H., Jara, C., Larama, G., Matus, F., 2023. Microbial response to warming and cellulose addition in a maritime Antarctic soil. Permafr. Periglac. Process.
Ramm, E., Liu, C., Ambus, P., Butterbach-Bahl, K., Hu, B., Martikainen, P.J., Marushchak, M.E., Mueller, C.W., Rennenberg, H., Schloter, M., 2022. A review of the importance of mineral nitrogen cycling in the plant-soil-microbe system of permafrost-affected soils—changing the paradigm. Environ. Res. Lett. 17, 013004.
Rantanen, M., Karpechko, A.Y., Lipponen, A., Nordling, K., Hyvärinen, O., Ruosteenoja, K., Vihma, T., Laaksonen, A., 2022. The Arctic has warmed nearly four times faster than the globe since 1979. Commun. Earth Environ. 3, 168.
Ravn, N.R., Elberling, B., Michelsen, A., 2020. Arctic soil carbon turnover controlled by experimental snow addition, summer warming and shrub removal. Soil Biol. Biochem. 142.
Revelle, W., Revelle, M.W., 2015. Package 'psych'. The comprehensive R archive network 337.
Richardson, J., Chatterjee, A., Jenerette, G.D., 2012. Optimum temperatures for soil respiration along a semi-arid elevation gradient in southern California. Soil Biol. Biochem. 46, 89–95.
Rodeghiero, M., Cescatti, A., 2005. Main determinants of forest soil respiration along an elevation/temperature gradient in the Italian Alps. Glob. Chang. Biol. 11, 1024–1041.
Schaefer, K., Jafarov, E., 2016. A parameterization of respiration in frozen soils based on substrate availability. Biogeosciences 13, 1991–2001.
Schimel, J.P., Bilbrough, C., Welker, J.M., 2004. Increased snow depth affects microbial activity and nitrogen mineralization in two Arctic tundra communities. Soil Biol. Biochem. 36, 217–227.
Schimel, J.P., Mikan, C., 2005. Changing microbial substrate use in Arctic tundra soils through a freeze-thaw cycle. Soil Biol. Biochem. 37, 1411–1418.
Schindlbacher, A., de Gonzalo, C., Díaz-Pinés, E., Gorría, P., Matthews, B., Inclán, R., Zechmeister-Boltenstern, S., Rubio, A., Jandl, R., 2010. Temperature sensitivity of forest soil organic matter decomposition along two elevation gradients. J. Geophys. Res. Biogeo. 115.
Shahi, S., Abermann, J., Silva, T., Langley, K., Larsen, S.H., Mastepanov, M., Schöner, W., 2023. The importance of regional sea-ice variability for the coastal climate and near-surface temperature gradients in Northeast Greenland. Weather Clim. Dyn. 4, 747–771.
Soong, J.L., Cotrufo, M.F., 2015. Annual burning of a tallgrass prairie inhibits C and N cycling in soil, increasing recalcitrant pyrogenic organic matter storage while reducing N availability. Glob. Chang. Biol. 21, 2321–2333.
Starr, G., Oberbauer, S.F., Ahlquist, L.E., 2008. The photosynthetic response of Alaskan tundra plants to increased season length and soil warming. Arct. Antarct. Alp. Res. 40, 181–191.
Sullivan, P.F., Stokes, M.C., McMillan, C.K., Weintraub, M.N., 2020. Labile carbon limits late winter microbial activity near Arctic treeline. Nat. Commun. 11, 4024.
Sun, Q., Wang, R., Hu, Y., Yao, L., Guo, S., 2018. Spatial variations of soil respiration and temperature sensitivity along a steep slope of the semiarid Loess Plateau. PLoS One 13, e0195400.
Team, R.C., 2019. R: A language and environment for statistical computing (Version 3.6. 1)[Software package]. Vienna, Austria: R Foundation for Statistical Computing. Retrieved from ….
Treharne, R., Bjerke, J.W., Tømmervik, H., Stendardi, L., Phoenix, G.K., 2019. Arctic browning: Impacts of extreme climatic events on heathland ecosystem CO_2 fluxes. Glob. Chang. Biol. 25, 489–503.
Tsui, C.-C., Chen, Z.-S., 2010. Net nitrogen mineralization and nitrification of different landscape positions in a lowland subtropical rainforest in Taiwan. Soil Sci. Plant Nutr. 56, 319–331.
Turner, M.G., Smithwick, E.A., Metzger, K.L., Tinker, D.B., Romme, W.H., 2007. Inorganic nitrogen availability after severe stand-replacing fire in the Greater Yellowstone ecosystem. Proc. Natl. Acad. Sci. 104, 4782–4789.
Vanhala, P., Karhu, K., Tuomi, M., Björklöf, K., Fritze, H., Liski, J., 2008. Temperature sensitivity of soil organic matter decomposition in southern and northern areas of the boreal forest zone. Soil Biol. Biochem. 40, 1758–1764.
Virkkala, A.-M., Virtanen, T., Lehtonen, A., Rinne, J., Luoto, M., 2018. The current state of CO_2 flux chamber studies in the Arctic tundra: a review. Prog. Phys. Geogr.: Earth Environ. 42, 162–184.
Watts, J.D., Natali, S.M., Minions, C., Risk, D., Arndt, K., Zona, D., Euskirchen, E.S., Rocha, A.V., Sonnentag, O., Helbig, M., 2021. Soil respiration strongly offsets carbon uptake in Alaska and Northwest Canada. Environ. Res. Lett. 16, 084051.
Welker, J.M., Fahnestock, J.T., Henry, G.H., O'Dea, K.W., Chimner, R.A., 2004. CO_2 exchange in three Canadian High Arctic ecosystems: response to long-term experimental warming. Glob. Chang. Biol. 10, 1981–1995.
Whitaker, J., Ostle, N., Nottingham, A.T., Ccahuana, A., Salinas, N., Bardgett, R.D., Meir, P., McNamara, N.P., 2014. Microbial community composition explains soil respiration responses to changing carbon inputs along an A ndes-to-A mazon elevation gradient. J. Ecol. 102, 1058–1071.
Xu, W., Lambæk, A., Holm, S.S., Furbo-Halken, A., Elberling, B., Ambus, P.L., 2021a. Effects of experimental fire in combination with climate warming on greenhouse gas fluxes in Arctic tundra soils. Sci. Total Environ. 795, 148847.
Xu, W., Prieme, A., Cooper, E.J., Mörsdorf, M.A., Semenchuk, P., Elberling, B., Grogan, P., Ambus, P.L., 2021b. Deepened snow enhances gross nitrogen cycling among Pan-Arctic tundra soils during both winter and summer. Soil Biol. Biochem. 160.
Xu, W., Frendrup, L.L., Michelsen, A., Elberling, B., Ambus, P.L., 2023. Deepened snow in combination with summer warming increases growing season nitrous oxide emissions in dry tundra, but not in wet tundra. Soil Biol. Biochem. 180.
Xu, X., Zhou, Y., Ruan, H., Luo, Y., Wang, J., 2010. Temperature sensitivity increases with soil organic carbon recalcitrance along an elevational gradient in the Wuyi Mountains, China. Soil Biol. Biochem. 42, 1811–1815.
Zeeman, M.J., Hiller, R., Gilgen, A.K., Michna, P., Plüss, P., Buchmann, N., Eugster, W., 2010. Management and climate impacts on net CO_2 fluxes and carbon budgets of three grasslands along an elevational gradient in Switzerland. Agric. For. Meteorol. 150, 519–530.
Zhang, Z.-S., Dong, X.-J., Xu, B.-X., Chen, Y.-L., Zhao, Y., Gao, Y.-H., Hu, Y.-G., Huang, L., 2015. Soil respiration sensitivities to water and temperature in a revegetated desert. J. Geophys. Res. Biogeol. 120, 773–787.
Zhang, Y., Liu, S., Cheng, Y., Cai, Z., Müller, C., Zhang, J., 2019. Composition of soil recalcitrant C regulates nitrification rates in acidic soils. Geoderma 337, 965–972.
Zona, D., Lipson, D., Zulueta, R., Oberbauer, S., Oechel, W., 2011. Microtopographic controls on ecosystem functioning in the Arctic Coastal Plain. J. Geophys. Res. Biogeol. 116.